RSC Advances

This article can be cited before page numbers have been issued, to do this please use: M. Niazi, H. R. Shahsavari, M. Golbon Haghighi, M. R. Halvagar, S. Hatami and B. Notash, *RSC Adv.*, 2016, DOI: 10.1039/C6RA21756G.

ROYAL SOCIETY OF CHEMISTRY

www.rsc.org/advances

View Article Online
DOI: 10.1039/C6RA21756G

Carbon–Sulfur Bond Reductive Coupling from a Platinum(II) Thiolate Complex

Maryam Niazi,[a] Hamid R. Shahsavari,[a] Mohsen Golbon Haghighi,[b] Mohammad Reza Halvagar,[c] Samaneh Hatami[a] and Behrouz Notash[b]*

[a]Department of Chemistry, Institute for Advanced Studies in Basic Sciences (IASBS), Yousef Sobouti Blvd., Zanjan 45137-6731, Iran.

[b]Department of Chemistry, Shahid Beheshti University, Evin, Tehran 19839-69411, Iran

[c]Chemistry & Chemical Engineering Research Center of Iran, Tehran,14968-13151, Iran

Email: shahsavari@iasbs.ac.ir

Abstract

The room temperature addition of electrophilic alkyl halide reagents (RX = MeI, EtI and $PhCH_2Br$) to complex [Pt(ppy)(η^1-S-Spy)(PPh_3)], **1a**, in which ppyH = 2-phenylpyridine and pySH = pyridine-2-thiol, resulted in a rapid Carbon–Sulfur (C–S) bond reductive coupling to produce alkyl sulfides and corresponding halide complexes [Pt(ppy)(PPh_3)X], X = I (**2a**) and Br (**2b**). A mechanism for this C–S bond formation reaction was suggested based on ^1H and $^{31}P\{^1H\}$ NMR spectroscopic analyses. In the suggested mechanism, the reaction proceeded through a binuclear intermediate complex [{Pt(ppy)(PPh_3)}$_2$(μ_2-Spy)]I, **3-I**, which was separately synthesized by another counter anion (PF_6) and it was fully characterized by multinuclear NMR spectroscopy and single X-ray crystallography. Also, density functional theory (DFT) calculations were used to theoretically assess the structures of intermediates and transition states in this bond formation reaction.

Introduction

Several prominent catalytic or stoichiometric systems were developed for C–H,[1, 2] C–C[2-8] and C–X[8-17] (X = different heteroatoms) bond formation reactions. Despite these extensive research efforts, C–S bond formation still has significant limitations identical to poisoning

View Article Online
DOI: 10.1039/C6RA21756G

and/or deactivation effect of sulfur on reactive species or harsh reaction conditions.[14-16] Such difficulties were addressed in some cases and numerous outstanding systems were established for C–S bond coupling[16] using transition metals such as Ni,[18] Cu,[17] Pd[8, 16] and Pt.[19] In addition, the growing interest in C–S bond construction chemistry is mostly due to its potential applications in organic synthesis,[20] materials science,[21] agricultural,[15] and pharmaceutical industry.[22]

There are only a few reports on the formation of C–S bond using platinum transition metal complexes.[19] This fact has led us to apply complex [Pt(ppy)(η^1-S-Spy)(PPh_3)], **1a**, ppyH = 2-phenylpyridine and pySH = pyridine-2-thiol, in C–S bond reductive coupling with electrophilic reagents such as alkyl halides at room temperature. In addition, mechanistic aspect of this bond formation reaction was studied with multinuclear NMR spectroscopy by observing an interesting binuclear complex. Density functional theory (DFT) was employed to optimize structures of the related complexes, which were observed experimentally or proposed theoretically.

Result and Discussion

Complex [Pt(ppy)(η^1-S-Spy)(PPh_3)], **1a**, was prepared according to our recently published procedure (Scheme 1 (path I)), [23] involving treatment of complex [Pt(ppy)(PPh_3)Cl], **A**,[24] with an ethanolic solution of sodium pyridine-2-thiolate (NaC_5H_4NS) under Ar atmosphere.

The reaction of complex **1a** with stoichiometric ratio or an excess of MeI at room temperature was investigated. This reaction was extremely rapid and yielded unexpected products. As represented in Scheme 1 (path II), the reaction underwent fast C–S bond reductive coupling to cleanly produce an organic compound 2-(methylthio)pyridine (pySMe), **O1**,[25] and complex [Pt(ppy)(PPh_3)I], **2a**.

View Article Online
DOI: 10.1039/C6RA21756G

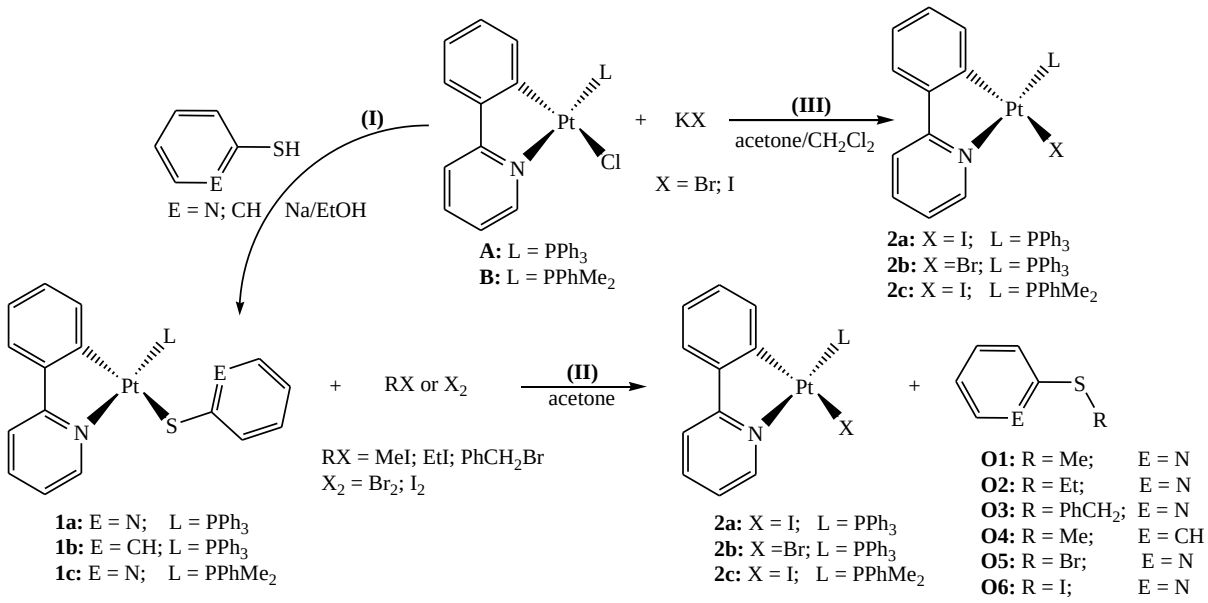

Scheme 1. (I) the synthetic route for the formation of complexes **1**; (II) identified products in the reaction of different alkyl halides with complexes **1**; (III) direct route for the formation of complexes **2** by halide substitution. All reactions were carried out under inert atmosphere at room temperature.

Complex **2a** was identified from the analysis of NMR spectroscopy data and X-ray single crystal diffraction data (see structural determination). As expected, the $^{31}P\{^{1}H\}$ NMR spectrum of complex **2a** (in $CDCl_3$) displayed only a singlet along with platinum satellites at $\delta = 22.7$ with a significant value of $^{1}J_{PtP} = 4290$ Hz. This large coupling constant confirmed that the phosphine ligand is positioned *trans* to nitrogen atom, same as complex **A**.[24] In the ^{1}H NMR spectrum of complex **2a**, the existence of a doublet of doublet of doublets for H^2 of ppy ligand at $\delta = 10.55$ ppm with platinum satellites ($^{3}J_{PtH} = 30.9$ Hz) and also another doublet of doublet of doublets at $\delta = 6.67$ ppm accompanied by platinum satellites ($^{3}J_{PtH} = 52.1$ Hz) for H^9 of ppy ligand, confirmed that cyclometalating ligand was chelated in this complex (refer to the Experimental Section for signal assignments). The later resonance exhibited a C–H···π interaction, as detected in the single X-ray crystal structure of complex **2a**. In addition, complex **2a** could be achieved directly by a nucleophilic substitution reaction of chloride ligand in complex **A** by iodide (I^-) ion (Scheme 1 (path III)).

View Article Online
DOI: 10.1039/C6RA21756G

Other electrophilic substrates have been used to investigate the effect of these kind of reagents on the above reaction (Scheme 1 (path II)). The obtained products were similar to the resultant products from methyl iodide species. For example, addition of ethyl iodide (EtI) or benzyl bromide ($PhCH_2Br$) to complex **1a** resulted in products 2-(ethylthio)pyridine (pySEt), **O2**,[25] and complex **2a** or 2-(benzylthio)pyridine **O3**,[25] and complex [Pt(ppy)(PPh_3)Br], **2b**, respectively (Scheme 1 (path II)). Complex **2b** was fully characterized by NMR spectroscopy and single X-ray crystallography studies (see structural determination, Experimental Section). Furthermore, complex **2b** was obtained through salt metathesis reaction of complex **A** with KBr (Scheme 1 (path III)).

*Mechanism of C–S Coupling from Complexes **1***

In an effort to achieve more insight into the mechanism of reaction (carbon–sulfur bond formation) that was described in Scheme 1 (path II), it was monitored at different temperatures with NMR spectroscopy. The reactants were mixed and firstly NMR spectra were recorded at 25 °C. In ^{31}P {^1H} NMR spectra (Figure 1), immediately after addition of MeI, the signals of the starting complex **1a** (δ = 22.7 ppm) quickly disappeared (Figure 1c) and a signal corresponding to complex **2a** (δ = 22.4 ppm) grew rapidly as time elapsed. Apart from resonances of complex **1a** (precursor) and complex **2a** (product), an interesting Pt(II)-Pt(II) dinuclear intermediate species was detected, suggesting the presence of two different phosphorus ligands with high platinum coupling constants (Figure 1). Its structure was determined as a binuclear complex [{Pt(ppy)(PPh_3)}$_2$(μ_2-Spy)]I, **3-I**. Therefore, two singlet signals, one at δ = 21.5 ppm ($^1J_{PtP}$ = 4407 Hz, P^a) and another one at δ = 21.0 ppm ($^1J_{PtP}$ = 4245 Hz, P^b) were assigned to complex **3-I** and phosphine ligands in this complex perhaps were located in *cis* position to the nitrogen and sulfur atoms of bridging thiolate ligand, respectively. This assignment is related to high *cis* influence of S atom over N atom.[26, 27] As time passed, the signal intensities of complex **3-I** decreased while the signal intensities of complex **2a** increased until full conversion (*ca*. 6 h) was obtained as compared to the pure form of complex **2a**.

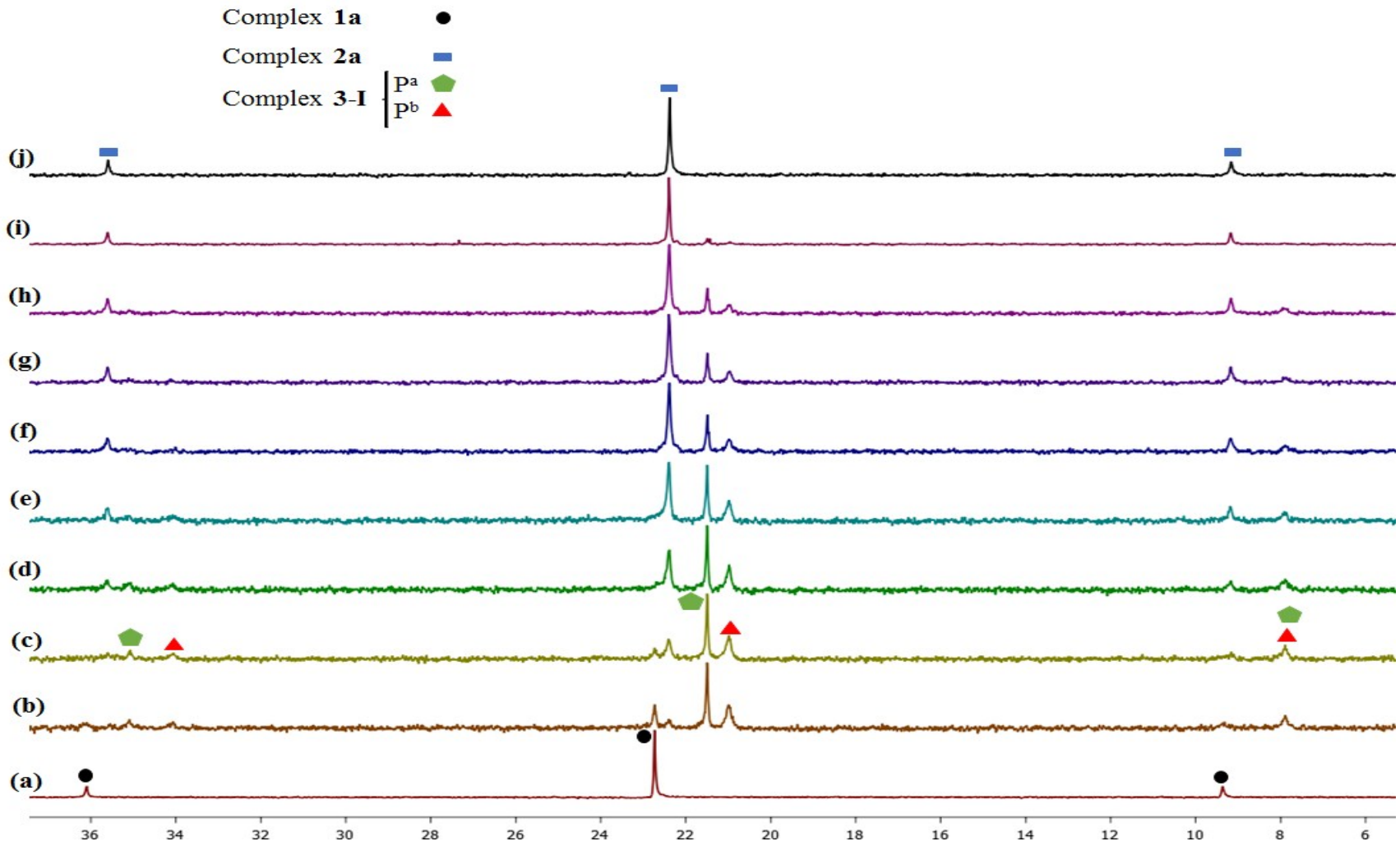

Figure 1. Reaction of complex **1a** with 3eq of MeI as monitored by $^{31}P\{^{1}H\}$ NMR spectroscopy in CD_2Cl_2 at room temperature. (a) Pure complex **1a**, (b) immediately after addition of MeI, (c) 5 min (d) 15 min, (e) 30 min, (f) 60 min, (g) 120 min, (h) 180 min, (i) 240 min and (j) 480 min. The signal assignments are shown.

View Article Online
DOI: 10.1039/C6RA21756G

The related ^{1}H NMR spectra (Figure S1) for this reaction were also obtained simultaneously at room temperature. This observation confirmed the formation of complex **2a**, and especially compound **O1**, as products and complex **3-I** as an intermediate by observing their expected signals. As shown in Figure S1, new resonances with increased signals at δ = 2.58 ppm and 8.46 ppm were assigned to methyl and $H^{6'}$ (CH group adjacent to nitrogen atom) of compound **O1**,[25] respectively. When complex **1** was treated with CD_3I under the same conditions (CD_2Cl_2, room temperature), the methyl signal disappeared in the ^{1}H NMR spectrum (Figure S2).

To detect other plausible intermediates, the reaction was monitored at low temperature (223 K). In this temperature the rate of reaction became very slow and an excess of MeI was used. However, no further intermediates were observed (Figure S3) and similar room temperature NMR spectra were obtained. This spectroscopic observation suggested that other possible intermediates were very short lived and they were quickly transformed to the products.

Attempts to prepare resemble of complex **3-I** were successful. The synthetic strategy involved treatment of complex **A** with $AgPF_6$ to abstract the chloride (Cl^-) ligand from the platinum center as AgCl (separated from solution by filtration). Subsequently, complex **1a** was added to the resulting solution and the binuclear complex [{Pt(ppy)(PPh_3)}$_2$(μ_2-Spy)]PF_6, **3-PF_6**, was formed as an orange solid. The multinuclear NMR spectroscopy and crystal structure determination confirmed the formation of this complex. The ^{31}P {^{1}H} NMR spectrum (Figure 2) of complex **3-PF_6** exhibited two singlet resonance flanked by platinum satellites at similar chemical shift (with equal coupling $^{1}J_{PtP}$ constant) of complex **3-I**. It is notable that the counteranion (I^- or PF_6^-) did not have impact effect on the cationic part of complex **3** in solution and only PF_6^- facilitated crystallization process. As expected, the ^{195}Pt {^{1}H} spectrum (Figure 2) of complex displayed two doublets at -4081 (Pt^a) and -4296 (Pt^b) ppm with $^{1}J_{PtP}$ values of 4413 and 4256 Hz, respectively, close to the values obtained from the ^{31}P {^{1}H} NMR spectrum.

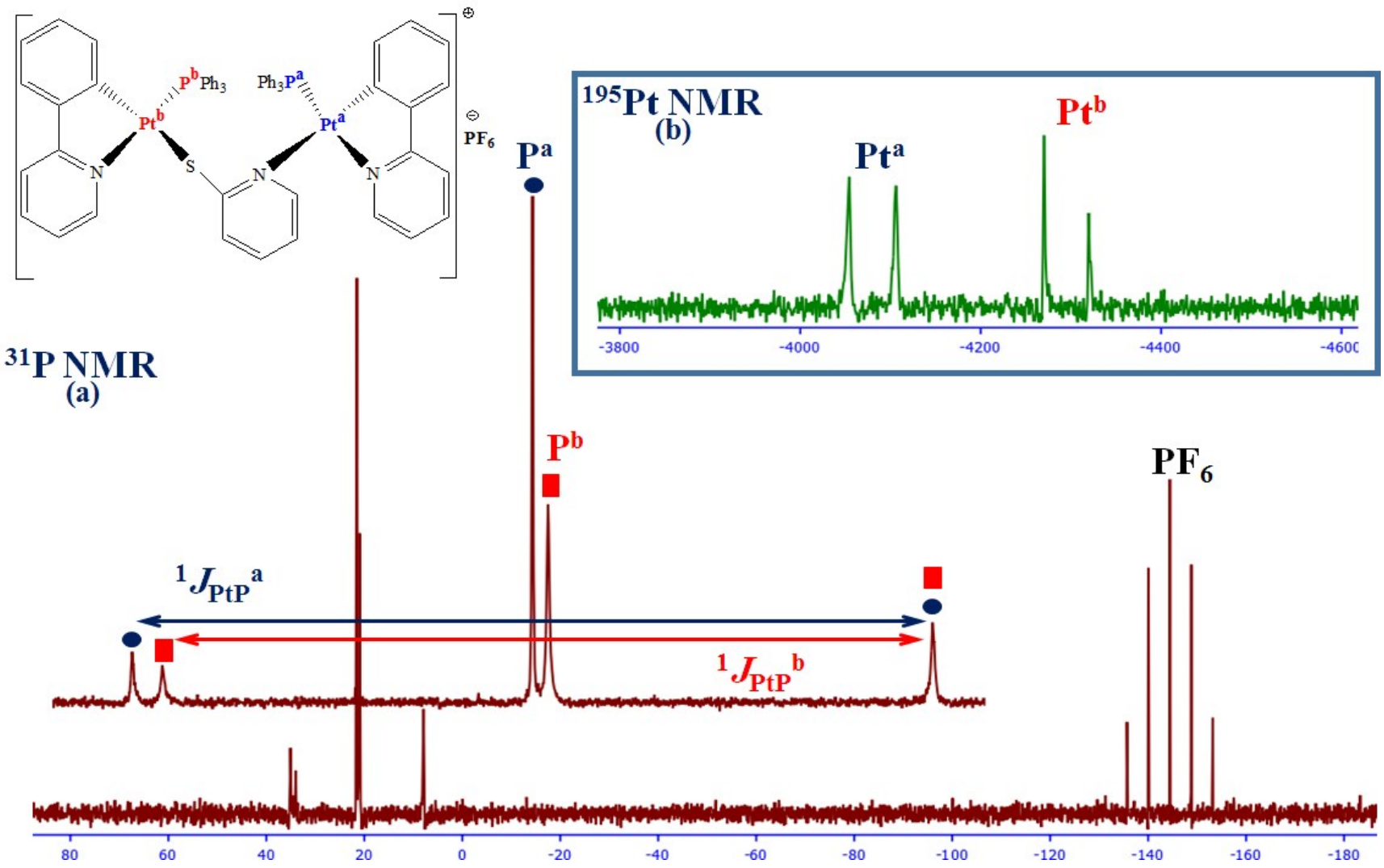

Figure 2. (a) ^{31}P and (b) ^{31}Pt NMR spectra of complex **3-PF$_6$** in CD_2Cl_2 at room temperature.

View Article Online
DOI: 10.1039/C6RA21756G

The synthesized complex **3-I** was stable in solution for several days and it did not display any decomposition products or rearrangements to complexes **1a** and **2a**. Also, complex **3-I** was treated with MeI and it easily was reacted and lead to complex **2a** and compound **O1**. When complex **3-PF6** was treated with MeI it did not show any reaction after six hours. According to this data, the binuclear complex **3**, perhaps, after the reaction with MeI and subsequent C–S bond coupling needs two coordinating anion like complex **3-I** (one from counterion and another from MeI). But complex **3-PF_6** has a non-coordination counterion (PF_6^-), probably, this point stops desire bond formation.

Initial coordination site of alkyl halide species in complex **1a** is important, because complex **1a** contains three potential sites (nitrogen, sulfur of Spy and platinum center) for initial coordination of alkyl halide reagents. Therefore, some tests were conducted to clarify the nucleophilicity of each coordination site in complex **1a** against these substrates (see below). The results from these experiments were helpful in proposing a mechanistic pathway for the observed C–S bond formation reaction in this study.

The free nitrogen of thiolate ligand in complex **1a** with alkyl halide reagents could potentially undergo Menschutkin reaction[28] to produce N-alkylated complexes (Scheme S1, Nitrogen path), although those were not observed in NMR spectroscopy studies (Figure S1). The possible N-methylated complex **1-N** from the reaction of complex **1a** with MeI could display a low field signal owing to the coordinated methyl on nitrogen.[26] Supposedly, cationic complex **1-N** was not stable and could not be detected with spectroscopic methods and it was converted to complex **2a** and compound **O1-t** (N-methyl-2-thiopyridone).[29] But, ^{1}H NMR spectra[29] did not show any signal for the formation of compound **O1-t** and only compound **O1** was observed. It is notable that the conversion of compound **O1-t** to compound **O1** (referenced to the thione-thiol tautomer)[29, 30] needs harsher reaction conditions.[29] To solve this challenge, complex [Pt(ppy)(SPh)(PPh_3)], **1b**,[23] in which PhSH = thiophenol, with no pendant nitrogen atom was selected for reaction with MeI.[31] This reaction produced complex **2** and its corresponding C–S coupling product *i.e.* thioanisole **O4**[32] (Scheme 1 (path II)). Therefore, this test suggested that the uncoordinated nitrogen atom does not have an important role in the

View Article Online
DOI: 10.1039/C6RA21756G

formation of yielded compounds and perhaps it has some effects on the formation of complex **3-I** from complex **1a**. Consequently, when the test reaction was followed with NMR spectroscopy (Figure S4 and Figure S5) it merely displayed transformation of complex **1b** to complex **2a** without any detectable intermediates in comparison with complex **1a** (Figure 1). All above observations suggested that the nitrogen site has weak nucleophilicity.[31] Comparable type of systems, each having at least one free nitrogen atom on the coordinated ligand to platinum center remain intact in reaction with alkyl halide because other sites of these complexes are stronger nucleophiles than N atom.[31, 33-35] Consequently, a different site in complexes **1a** and **1b** is involved in the initial coordination of alkyl halide reagents.

An alternative possibility for preliminary coordination of alkyl halides to complex **1a** is sulfur atom which is known as S-alkylation.[36-40] It is related to the metal complexes containing thiolate ligands especially dithiolate group,[38-41] while these are treated with alkyl halides species (in thermal condition for most cases)[38, 39, 42] S-alkylation is a plausible route.[36, 37, 43] As shown in Scheme S1 (Sulfur path), in the case of MeI, the presumed S-methylated complex **1-S** ought to exhibit a signal with platinum satellite in relation to coordinated methyl to sulfur atom but this was not observed (Figure S1). Thus, another experiment was designed for unravelling this inconsistency. While complex **1a** reacted with iodine or bromine reagents, it produced complexes **2a** or **2b** and its corresponding S–I or S–Br coupling products[44] (Scheme 1 (path II)). This reaction was followed by NMR spectroscopy and an intermediate (complex **3-I**) similar to the reaction of methyl iodide was detected (Figure 1). Therefore, sulfur atom is not incipient coordination site and S-alkylation can be ruled out.[43] Also, there are numerous reports on the oxidation of metal centers by alkyl substrates[45-48] than sulfur oxidation (thiolate alkylation). For example, Sicilia research group reported that the reaction of half-lantern compound (containing thiolate ligand) with MeI leaded to the oxidized complex and S-alkylation did not occur.[48] Therefore, the proposed routes in Scheme S1 are not appropriate and platinum center is initial coordination site for alkyl halide substrates and oxidative addition path is adequate for suggested C–S coupling mechanism (Scheme 2).

View Article Online
DOI: 10.1039/C6RA21756G

We also investigated the effect of phosphine ligand on the C–S bond formation by changing PPh_3 with $PPhMe_2$, and complex [Pt(ppy)(η^1-S-Spy)($PPhMe_2$)], **1c**, was prepared (Scheme 1 (path I)). When alkyl halide regent (MeI) was added to complex **1c** in acetone-d_6 at room temperature and the reaction was followed by NMR spectroscopy, rapid and complete conversion to complex [Pt(ppy)($PPhMe_2$)I], **2c**, and **O1** was observed (Scheme 1 (path II)). This reaction pathway is analogous to the reaction with complex **1a** which contains PPh_3, but C–S bond reductive elimination occurs at a faster rate. The increased rate of reaction is consistent with the greater nucleophilicity of complex **1c** than complex **1a**.[33, 49]

Structural Determination

Single-crystal X-ray diffraction investigation was carried out on complexes **A**, **2a**, **2b** and **3-PF$_6$** to approve their molecular structures. Crystallographic data are collected in Table S1, and selected bond distances and angles are quoted in Table S2. The perspective drawing of these complexes are illustrated in Figure 3 and Figure S6.

All complexes **A**, **2a**, **2b** and **3-PF$_6$** reveal a distorted square planar coordination environment around Pt(II) center. This distortion is due to small bite angle [81.0(5)–78.7(13)^o] of the ppy cyclometalated ligand. This narrow bite angle with bond distances for cyclometalated chelate (*i.e.* Pt-C_{ppy} and Pt-N_{ppy}) are comparable to those observed in other five membered rings of 2-phenylpyridinate platinum(II) complexes.[50-53] In each structure, the metalated carbon atom of the ppy ligand accommodates the coordinated phosphine ligand in *cis* arrangement of Pt–C_{ppy} bond, as a result of high *trans* influence of carbon atom.[54] Therefore, PPh_3 ligands are located *trans* to nitrogen atom of ppy ligand and bond distances of the Pt–P are notably shorter than platinum–phosphorous bond lengths, positioned *trans* to carbon atom of cyclometalated ligand.[50] Furthermore, halogen ligand completes the coordination sphere of platinum atom in complexes **A**, **2a** and **2b** or nitrogen and sulfur atoms of bridging Spy ligand in complex **3-PF$_6$**. Also, in binuclear complex **3-PF$_6$** the pyridine-2-thiolate group acts as a bridging ligand and binds two Pt centers through S^N coordination. The nitrogen and sulfur atoms of Spy ligand in this complex occupies a position *trans* to the Pt–C_σ bond of cyclometalated ligands.

View Article Online
DOI: 10.1039/C6RA21756G

Additional examination on the molecular packing of the crystal structures displayed the presence of inter- and intramolecular interactions (see below) such as C–H···π interaction, π···π stacking, without any notable Pt···Pt contacts. All molecular structures reveal a moderate short C–H···π intramolecular interaction (Figure S7) between hydrogen atom adjacent to coordinated carbon atom of cyclometalated ligand and the phenyl ring of the triphenylphosphine ligand (C–H···π; C2···C_{ph} (PPh_3) = 3.320-3.416 Å (**A**), 3.237-3.401 Å (**2a**), 3.291-3.365 Å (**2b**), for **3-PF$_6$**, C–H···π; C11 or C45···C_{ph} (PPh_3) = 3.244-3.493 Å, C–H···π; C1···C_{Spy} = 3.462 Å).

The crystal structure of complexes **A**, **2a** and **2b** shows that the halogen ligand is involved in a substantial intramolecular interaction with C–H group adjacent to coordinated nitrogen atom of ppy ligand (Figure S8). This C–H···X interaction causes deshielding of the proton involved in hydrogen bonding[55, 56] (~ 1.3 to 1.9 ppm) in ^{1}H NMR (Figure S9) relative to the hydrogen in free ppy ligand.[57] The shift values has also increased according to atomic radii of halogen ligands in the order of Cl < Br < I.[58]

In complex **3-PF$_6$** the ring of the pyridine-2-thiolate ligand exhibits weak intramolecular π···π interaction with one of the phenyl groups of the PPh_3 ligand bound to the Pt1 with distance between the centroids of 3.888 Å (Figure S10). Complexes **A** and **2b** are stacked through short intermolecular π···π interactions with an inter-planar distance of 3.335 Å and 3.329 Å, respectively. These interactions lead to formation of a dimer in a head to tail style, which are analogous to other platinum complexes having ppy fragments[51] (Figure S11). Furthermore, in crystal network of complex **2b**, each Br atom is bound to one hydrogen atom of the phosphine ligand from neighboring unit. In this molecular structure, each Pt(ppy) moiety is arranged through π···π interactions with another Pt(ppy) fragment in nearby chain and thus giving rise to a 2D network (Figure S12). Therefore, this complex indicates that the C–H groups (see above discussion) are involved in the formation of intra- and intermolecular hydrogen bonds[59] through the coordinated Br ligand with bond distance of 2.583 Å and 3.045 Å, respectively (Figure S8c and Figure S12). Complex **2a** displays the comparatively long interlayer distances between nearby ppy ligands that are longer than 3.8 Å,[60] demonstrating the lack of π···π interactions in this complex.

View Article Online
DOI: 10.1039/C6RA21756G

DFT Investigation

In order to verify this approach (according to the experimental data), we calculated the energy and reaction profiles for the oxidative addition of Me–I to complex **1a** and carbon–sulfur bond formation from the suggested intermediate structures (Scheme 2 and Figure 4). It is also worth mentioning that the pyridyl group and its peripheral nitrogen donor atom could be orientated in four different fashions (Figure S13). In these modes, the py ring and N atom are located at a plane above or below of the molecule and near or far from the platinum center, respectively. However, theoretical calculations suggest all possible orientations have small variation in energy (~ 2 KJ mol^{-1}), perhaps due to free rotation around S–C_{py} bond.[61] But, the form **a** (Figure S13) is preferred over other structures since it is in good agreement with further theoretical calculations (see below).

The DFT calculations suggest that the electron rich platinum center of complex **1a** (as a nucleophile) attacks on carbon atom of MeI (as an electrophile) to form transition state **TS1** and energy barrier for this state is +52.9 KJ mol^{-1}. This transition state illustrates a linear arrangement for I···C_{MeI}···Pt with the bond angles close to 90˚ and 180˚ between H–C_{MeI}···Pt (90-93˚) and I···C_{MeI}···Pt (178.5˚), respectively. The most important modifications in bond distances are detected for I···C_{MeI} and Pt···C_{MeI} in transition state **TS1**. These calculations suggested that the bond distance increases for I···C_{MeI} (2.73 Å) in this transition state as compared to MeI (2.20 Å), while Pt···C_{MeI} (2.49 Å) bond length is reduced.[62, 63] This data supports the hypothesis that the formation of transition state **TS1** is followed by concurrent bond breaking of methyl–iodide and a new bond formation between platinum and methyl, then the cationic 5-coordinate intermediate **IM1** is obtained. This intermediate is equilibrated with the comparable intermediate **IM2** with phosphine ligand and Me group being in *trans* disposition at platinum center (Figure 4). Both intermediates **IM1** and **IM2** could potentially convert to the 6-coordinate compounds **P1** and **P2**, respectively (Scheme 2). The calculation indicates that the energy barriers for these compounds are high (+42.9 and +50.3 KJ mol^{-1} for compounds **P1** and **P2**, respectively) and subsequent C–S bond coupling is not favorable. It is recommended that this concerted elimination from the five-coordinate d^6 metal complexes is more straightforward

View Article Online
DOI: 10.1039/C6RA21756G

than direct elimination from the saturated six-coordinate metal complexes.[11, 64, 65] Therefore, the carbon–sulfur bond formation from intermediate **IM1** (selected based on its good agreement with theoretical calculations) proceeds via transition state **TS2** as a concerted reductive elimination[66] (Scheme 2). In **TS2**, the bond distances between platinum with methyl (2.42 Å) or thiolate (2.47 Å) groups are lengthened and the bond angle of C_{Me}–Pt–S_{Spy} (61.3˚) is decreased and it suggested that this elimination is appropriate. Another possibility for the reductive elimination of C–S bond, probably, is the microscopic reverse of the popular S_N2 mechanism.[66, 67] In this mechanism, pervious mechanistic evidences provided, the nucleophilic groups like NR^-, OR^-, I^- dissociated from central metal, and then perform S_N2 attack upon an alkyl ligand (Me group) of the cationic intermediates.[12, 65, 68-70] Therefore, by addition of excess of nucleophilic groups to the reaction mixture the rate of reaction should be increased. By this strategy, when Spy^- was added to the reaction mixture, the desire C–S bond coupling reaction was stopped. Due to Spy^- was reacted with MeI and compound **O1** and KI salt were formed without accelerating rate of reductive elimination of C–S from intermediate **IM1**. Consequently, the possibility of S_N2 mechanism is not proper for this C–S bond formation. As compound **O1** dissociates from this transition state (**TS2**), the new cationic T-shaped intermediate **IM3**[11, 65, 69, 71] is produced (Scheme 2). Intermediate **IM3** can then react by two routes: (i) migration of iodide to the platinum center and formation of complex **2a** as a very stable complex (-71.3 KJ), or (ii) reaction with complex **1a** to yield a cationic complex **3-I**. The latter pathway is slower (deduced from NMR, Figure 1 and Figure S1) and more favorable (-51.8 KJ, Figure 4). Subsequently, complex **3-I** in the presence of MeI acts as a nucleophile (perhaps through a classical S_N2 mechanism)[48] and leads to the formation of an intermediate **IM4**[48] (Pt(II)-Pt(IV)–Me). Finally, intermediate **IM4** through a reductive elimination process (Me–Spy, compound **O1**) generates the stable final products (Figure 4 and Scheme 2).

View Article Online
DOI: 10.1039/C6RA21756G

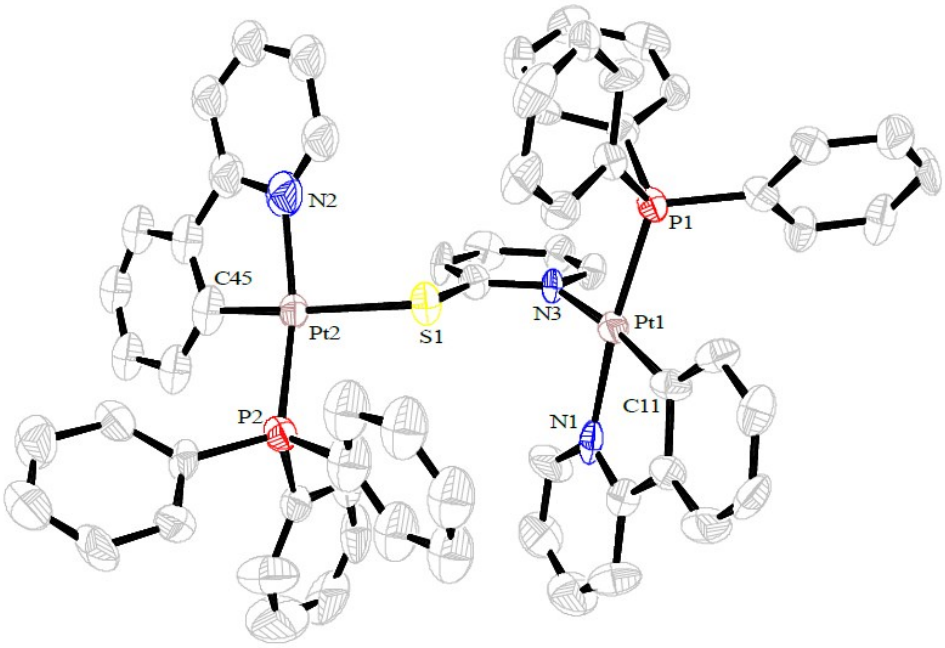

Figure 3. Representations of the X-ray crystal structure of complex [{Pt(ppy)(PPh_3)}$_2$(μ_2-Spy)]PF_6, **3-PF_6**, showing all non-hydrogen atoms as 40% thermal ellipsoids. Hydrogen atoms, PF_6 and a CH_2Cl_2 solvent molecule have been omitted for clarity. Pt1–C11 1.982(14), Pt2–C45 2.000(17), Pt1–N1 2.070(12), Pt2–N2 2.066(12), Pt1–N3 2.117(11), Pt1–P1 2.235(3), Pt2–P2 2.226(3), Pt2–S1 2.418(4), C11–Pt1–N1 81.0(5), C45–Pt2–N2 80.4(6), C11–Pt1–P1 95.0(4), C45–Pt2–P2 97.9(5), C11–Pt1–N3 172.2(4), C45–Pt2–S1 160.4(5), N1–Pt1–P1 173.5(3), N2–Pt2–P2 165.7(4), N1–Pt1–N3 91.2(4), N2–Pt2–S1 94.6(4), N3–Pt1–P1 92.8(3), P2–Pt2–S1 91.41(13).

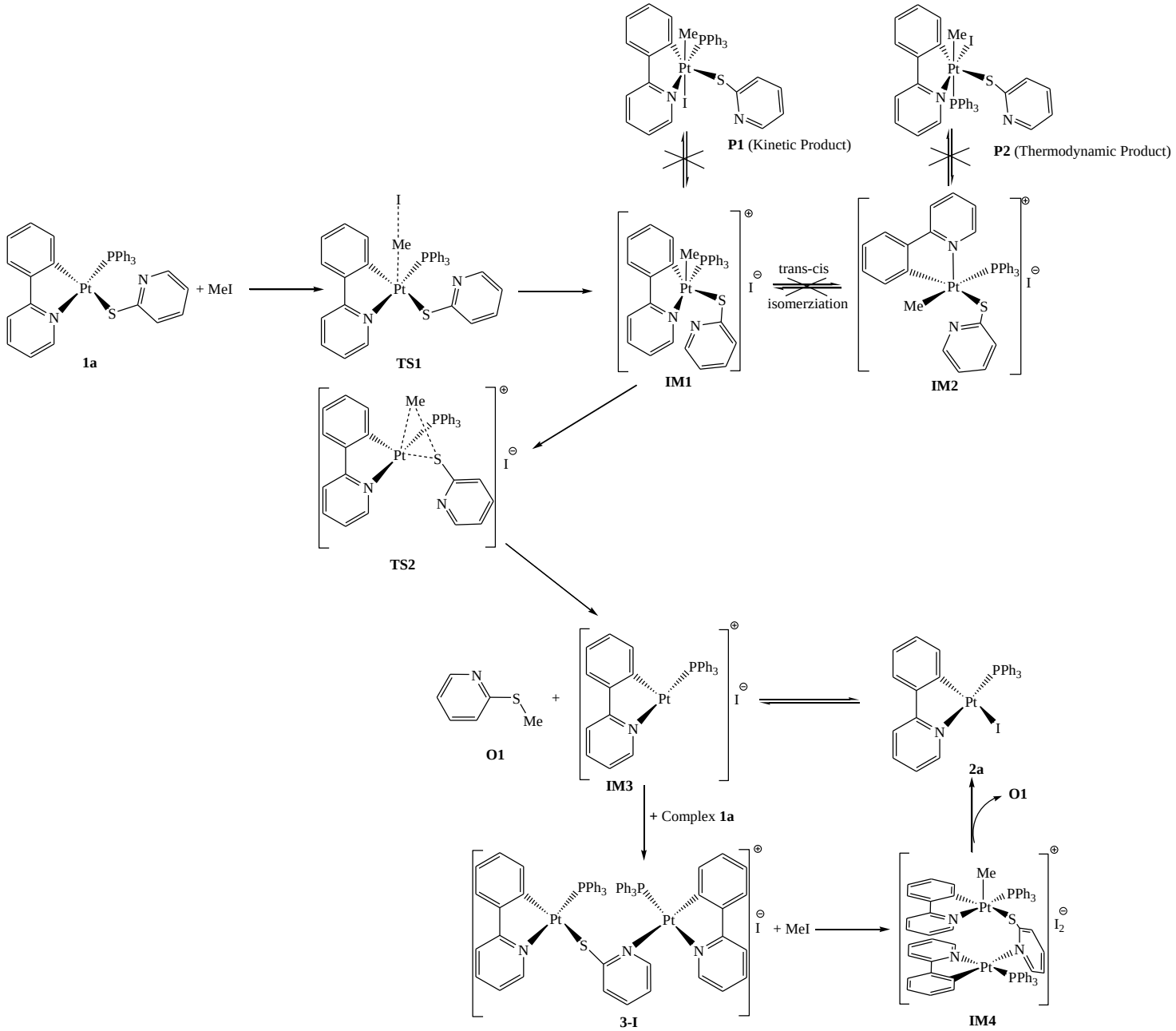

Scheme 2. Proposed mechanism for the reaction of complex **1a** with methyl iodide.

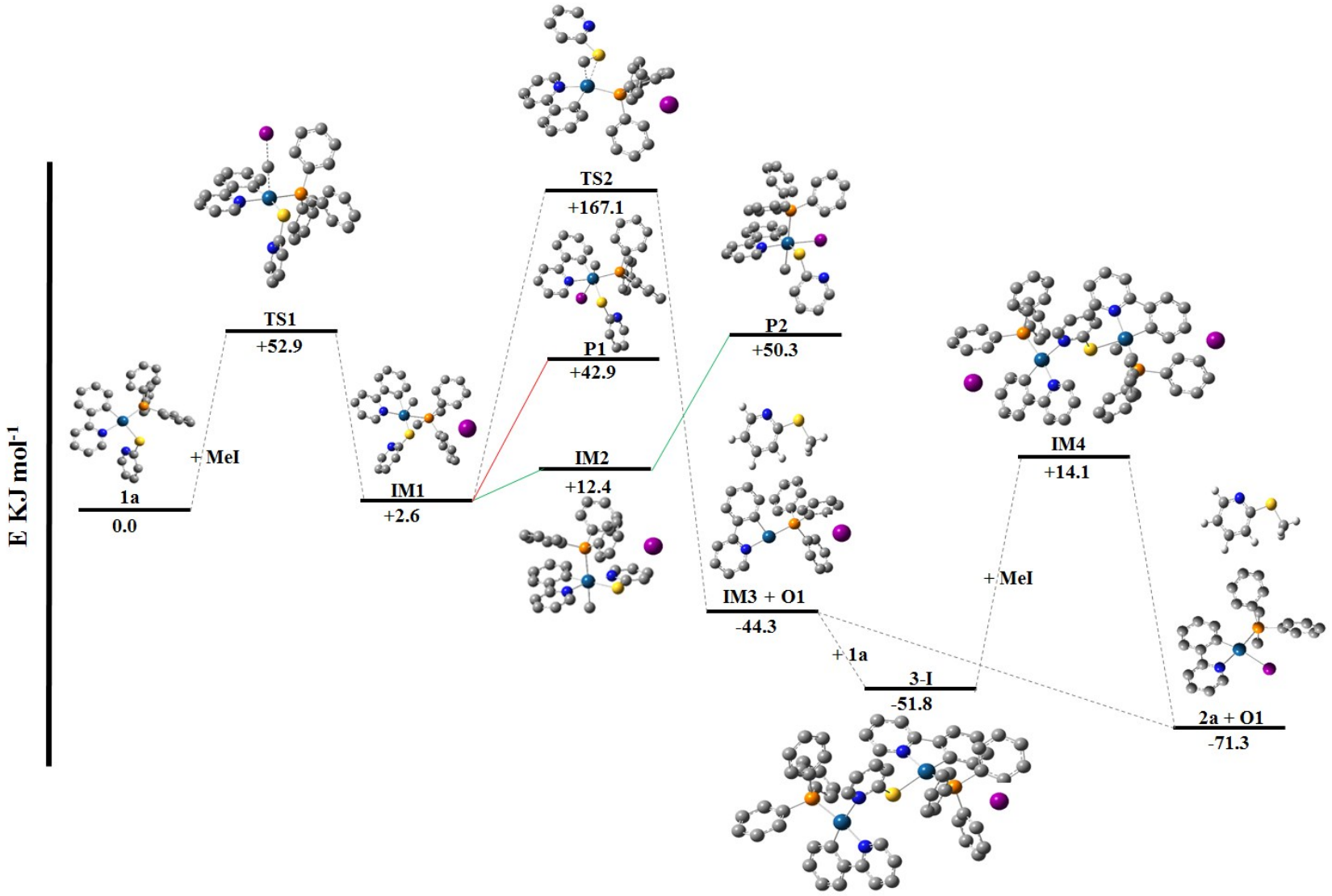

Figure 4. Calculated structures and relative energies for probable intermediates and transition states arising from the reaction of complex **1** and MeI in acetone solution.

View Article Online
DOI: 10.1039/C6RA21756G

Conclusion

The platinum(II) complex **1a** reacted readily with electrophilic alkyl sources at ambient temperature and through carbon–sulfur reductive coupling reaction produced corresponding halide complexes **2a** or **2b** and alkyl sulfides. This reaction was monitored by NMR spectroscopy at different temperatures and the results revealed (Scheme 2) an interesting binuclear complex **3-I** was formed during this process. Also, we proposed that the platinum center is a stronger nucleophile than peripheral nitrogen or sulfur atom. This claim was approved by selection of complex **1c**, which lacks a free nitrogen atom, and it underwent a similar C–S bond formation reaction. Moreover, in this experiment complex **1a** did not display any Pt(IV) compound(s) and perhaps such intermediate(s) is(are) energetically unfavorable as supported by DFT calculations. Therefore, platinum-thiolate complexes of these nature served as an appropriate platform for oxidative addition reaction that impressively enhanced the formation of alkyl sulfides.

Experimental Section

General procedures and materials

All NMR spectra (^{1}H, ^{31}P {^{1}H} and ^{195}P {^{1}H}) were recorded on a Brucker Avance DPX 400 MHz instrument. References were TMS or the residual peak of the solvent, *i.e.* CD_2Cl_2, $CDCl_3$ and acetone-d_6 (^{1}H), 85% H_3PO_4 (^{31}P), and aqueous Na_2PtCl_6 (^{195}Pt). The chemical shifts (δ) being reported as ppm and coupling constants (*J*) expressed in Hz. The microanalyses were performed using a vario EL CHNS elemental analyzer. Electrospray ion mass spectrum (ESI-MS) was recorded by a HP-5989B spectrometer using methanol–water as the mobile phase. All solvents were purified and dried according to standard procedures.[72] 2-phenylpyridine (ppyH), pyridine-2-thiol (pySH), thiophenol (PhSH), silver hexafluorophosphate ($AgPF_6$), triphenylphosphine (PPh_3) and dimethylphenylphosphine ($PPhMe_2$) were purchased from Aldrich or Acros. Complexes [Pt(ppy)(DMSO)(Cl)],[53] [Pt(ppy)(PPh_3)Cl], **A**,[24] [Pt(ppy)(η^1-S-Spy)(PPh_3)], **1a**,[23] [Pt(ppy)(SPh)(PPh_3)], **1b**,[23] were prepared as reported in literature. The NMR labeling for all ligands are shown in Scheme 3 for clarifying the chemical shift assignments.

View Article Online
DOI: 10.1039/C6RA21756G

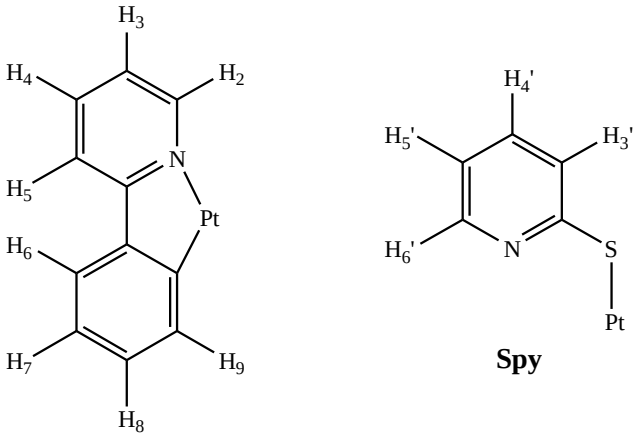

Scheme 3. Representative ligands with position labeling.

[Pt(ppy)(PPhMe$_2$)Cl], B.

To a solution of [Pt(ppy)(DMSO)Cl] (100 mg, 0.22 mmol) in acetone (10 mL) was added $PPhMe_2$ (30.8 μL, 0.22 mmol). The mixture was stirred at room temperature for 1 h. Then, the solvent was removed under reduced pressure and the residue was triturated with *n*-hexane (3 × 2 mL) and the resultant yellow solid was dried under vacuum. Yield: 94 mg, 83%. Elem. Anal. Calcd for $C_{19}H_{19}ClNPPt$ (522.87): C, 43.64; H, 3.66; N, 2.68; Found: C, 43.91; H, 3.74; N, 2.57. ^{1}H NMR (400 MHz, acetone-d_6, 20 °C, δ): 9.80 (d, $^3J_{PtH}$ = 24.1, $^3J_{HH}$ = 5.8, 1H, H^2), 8.11-8.04 (m, 4H, H^4, H^5 and H^o of $PPhMe_2$), 7.69 (dd, $^3J_{HH}$ = 7.8, $^4J_{HH}$ = 1.3, 1H, H^6), 7.53-7.48 (m, 4H, H^3, H^p and H^m of $PPhMe_2$), 7.00 (td, $^3J_{HH}$ = 7.8, $^4J_{HH}$ = 1.2, 1H, H^7), 6.87 (d, $^3J_{PtH}$ = 56.1, $^3J_{HH}$ = 7.8, 1H, H^9), 6.75 (td, $^3J_{HH}$ = 7.8, $^4J_{HH}$ = 1.2, 1H, H^8), 2.00 (d, $^2J_{PH}$ = 10.4, $^3J_{PtH}$ = 39.7 Hz, 6H, Me group of $PPhMe_2$). ^{31}P {^{1}H} NMR (162 MHz, acetone-d_6, 20 °C, δ): -8.1 (s, $^1J_{PtP}$ = 4131, 1P).

[Pt(ppy)(η^1-S-Spy)(PPhMe$_2$)], 1c.

Complex **B** (100 mg, 0.19 mmol) was added to an ethanolic solution of sodium pyridine-2-thiolate ligand (NaC_5H_4NS) under inert atmospheric condition [Note: NaC_5H_4NS was prepared by dissolving sodium (5.8 mg, 0.25 mmol) in 10 mL of absolute ethanol and subsequent treatment with pyridine-2-thiol (21.3 mg, 0.19 mmol)]. The resulting orange colored mixture was allowed to react while stirring for 12 h. Then, solvent was removed under reduced pressure

View Article Online
DOI: 10.1039/C6RA21756G

the residue was extracted with CH_2Cl_2 (20 mL). The obtained orange solution was filtered through Celite and the filtrate was concentrated to a small volume (1 mL). Finally, *n*-hexane (5 mL) was added to precipitate complex **1c** as an orange solid. Yield: 71 mg, 62%. Elem. Anal. Calcd for $C_{24}H_{23}N_2PPtS$ (597.57): C, 48.24; H, 3.88; N, 4.69; Found: C, 47.96; H, 3.74; N, 4.76. ^{1}H NMR (400 MHz, acetone-d_6, 20 °C, δ): 10.05 (m, $^3J_{PtH}$ = 26.2, 1H, H^2), 8.15-8.03 (m, 5H, H^4, H^5, $H^{6'}$ and H^o of $PPhMe_2$), 7.90 (dd, $^3J_{HH}$ = 7.8, $^4J_{HH}$ = 1.0, 1H, H^6), 7.57 (d, $^3J_{HH}$ = 8.0, 1H, $H^{3'}$), 7.48-7.36 (m, 4H, H^3, H^p and H^m of $PPhMe_2$), 7.19 (td, $^3J_{HH}$ = 7.8, $^4J_{HH}$ = 1.9, 1H, H^7), 7.02 (t, $^3J_{HH}$ = 7.1, 1H, $H^{4'}$), 6.98 (d, $^3J_{PtH}$ = 46.1, $^3J_{HH}$ = 7.8, 1H, H^9), 6.80 (td, $^3J_{HH}$ = 7.8, $^4J_{HH}$ = 1.7, 1H, H^8), 6.71 (dd, $^3J_{HH}$ = 5.1, $^4J_{HH}$ = 0.9, 1H, $H^{5'}$), 2.01 (d, $^2J_{PH}$ = 10.9, $^3J_{PtH}$ = 40.1 Hz, 6H, Me group of $PPhMe_2$). ^{31}P {^{1}H} NMR (162 MHz, acetone-d_6, 20 °C, δ): -8.5 (s, $^1J_{PtP}$ = 4178, 1P).

[Pt(ppy)(PPh$_3$)I], 2a.

Method A: To a yellow suspension of complex **1a** (100 mg, 0.14 mmol) in acetone (15 mL) was added an excess of MeI (174.3 μL, 2.8 mmol, 20 equiv.) at room temperature. The color of the mixture turned red instantly and then the mixture was stirred for 2 h. Then, the solvent was removed under reduced pressure and the residue was triturated with *n*-hexane (3 × 2 mL). The resulting green solid was dried under vacuum. Yield: 82 mg, 78%; m.p. 225 ˚C. Elem. Anal. Calcd for $C_{29}H_{23}INPPt$ (738.03): C, 47.15; H, 3.14; N, 1.90; Found: C, 47.81; H, 3.37; N, 1.97. ^{1}H NMR (400 MHz, $CDCl_3$, 20 °C, δ): 10.55 (ddd, $^3J_{PtH}$ = 30.9, $^3J_{HH}$ = 5.8, $^4J_{HH}$ = 0.9, $^4J_{PH}$ = 4.3, 1H, H^2), 7.87-7.77 (m, 8H, H^4, H^5, H^o of PPh_3), 7.50 (dd, $^3J_{HH}$ = 7.9, $^4J_{HH}$ = 1.1, 1H, H^6), 7.43-7.34 (m, 9H, H^p and H^m of PPh_3), 7.20 (tdd, $^3J_{HH}$ = 7.3, $^4J_{HH}$ = 1.3, $^4J_{PH}$ = 1.4, 1H, H^3), 6.99 (td, $^3J_{HH}$ = 7.9, $^4J_{HH}$ = 0.9, 1H, H^7), 6.67 (ddd, $^3J_{PtH}$ = 52.1,$^3J_{HH}$ = 7.3, $^4J_{HH}$ = 0.8, $^4J_{PH}$ = 4.0, 1H, H^9), 6.52 (td, $^3J_{HH}$ = 8.0, $^4J_{HH}$ = 1.3, 1H, H^8). ^{31}P {^{1}H} NMR (162 MHz, $CDCl_3$, 20 °C, δ): 22.7 (s, $^1J_{PtP}$ = 4290, 1P). ^{1}H NMR (400 MHz, acetone-d_6, 20 °C, δ): 10.54 (ddd, $^3J_{PtH}$ = 31.1, $^3J_{HH}$ = 5.7, $^4J_{HH}$ = 1.0, $^4J_{PH}$ = 4.3, 1H, H^2), 8.13-8.11 (m, 2H, H^4, H^5), 7.86-7.81 (m, 6H, H^o of PPh_3), 7.70 (dd, $^3J_{HH}$ = 7.9, $^4J_{HH}$ = 1.4, 1H, H^6), 7.50-7.40 (m, 10H, H^3, H^p and H^m of PPh_3), 6.99 (td, $^3J_{HH}$ = 7.9, $^4J_{HH}$ = 1.1, 1H, H^7), 6.69 (ddd, $^3J_{PtH}$ = 52.7,$^3J_{HH}$ = 7.4, $^4J_{HH}$ = 0.8, $^4J_{PH}$ = 4.0, 1H, H^9), 6.49 (td, $^3J_{HH}$ = 79, $^4J_{HH}$ = 1.5, 1H, H^8). ^{31}P {^{1}H} NMR (162 MHz, acetone-d_6, 20

View Article Online
DOI: 10.1039/C6RA21756G

°C, δ): 22.8 (s, $^{1}J_{PtP}$ = 4296, 1P). ^{1}H NMR (400 MHz, CD_2Cl_2, 20 °C, δ): 10.49 (m, $^{3}J_{PtH}$ = not resolved, 1H, H^2), 7.92-7.78 (m, 8H, H^4, H^5, H^o of PPh_3), 7.53 (dd, $^{3}J_{HH}$ = 7.8, $^{4}J_{HH}$ = 1.1, 1H, H^6), 7.44-7.38 (m, 9H, H^p and H^m of PPh_3), 7.25 (t, $^{3}J_{HH}$ = 7.4, 1H, H^3), 7.00 (t, $^{3}J_{HH}$ = 7.9, 1H, H^7), 6.65 (dd, $^{3}J_{PtH}$ = 52.4,$^{3}J_{HH}$ = 7.5, $^{4}J_{PH}$ = 4.1, 1H, H^9), 6.52 (t, $^{3}J_{HH}$ = 7.9, 1H, H^8). ^{31}P {^{1}H} NMR (162 MHz, CD_2Cl_2, 20 °C, δ): 22.4 (s, $^{1}J_{PtP}$ = 4288, 1P).

Method B: To a yellow suspension of complex **1a** (100 mg, 0.14 mmol) in acetone (15 mL) was added a solution of I_2 (175.8 g, 0.70 mmol, 5 equiv.) in acetone (5 mL) at room temperature. A fast color change to red was observed. The resulting solution was stirred for 2 h. Then, the solvent was reduced under vacuum to a small volume (1 mL) and *n*-hexane (5 mL) was added to precipitate complex **2a** as a green powder (73 mg, 71%).

Method C: To a green suspension of complex **A** (100 mg, 0.15 mmol) in acetone/CH_2Cl_2 (10:5 mL) was added an excess of KI (74.7 g, 0.45 mmol, 3 equiv.) in acetone (2 mL) at room temperature. The resulting mixture was allowed to react while stirring for 24 h. Then, the solvent was removed under reduced pressure and the residue was extracted with CH_2Cl_2 (20 mL). The obtained green solution was filtered through Celite and the filtrate was concentrated to a small volume (1 mL). Finally, *n*-hexane (5 mL) was added to yield complex **2a** as a green solid which was dried under vacuum (48 mg, 43%).

[Pt(ppy)(PPh$_3$)Br], 2b.

Method A: To a yellow suspension of complex **1a** (100 mg, 0.14 mmol) in acetone (15 mL) was added benzyl bromide (166.3 μL, 1.4 mmol, 10 equiv.) at room temperature and an orange solution was obtained quickly. The reaction mixture was stirred for 2 h. Then, the solvent was evaporated under vacuum and the residue was washed with *n*-hexane (3 × 2 mL), resulting in a green solid which was dried under vacuum. Yield: 86 mg, 89%; m.p. 221 ˚C. Elem. Anal. Calcd for $C_{29}H_{23}BrNPPt$ (690.04): C, 50.43; H, 3.36; N, 2.03; Found: C, 51.01; H, 3.59; N, 2.26. ^{1}H NMR (400 MHz, $CDCl_3$, 20 °C, δ): 10.18 (ddd, $^{3}J_{PtH}$ = 30.8, $^{3}J_{HH}$ = 5.7, $^{4}J_{HH}$ = 1.0, $^{4}J_{PH}$ = 4.1, 1H, H^2), 7.89-7.77 (m, 8H, H^4, H^5, H^o of PPh_3), 7.51 (dd, $^{3}J_{HH}$ = 7.8, $^{4}J_{HH}$ = 1.2, 1H, H^6), 7.44-7.35 (m, 9H, H^p and H^m of PPh_3), 7.27 (m, 1H, H^3, this signal has overlapping with $CHCl_3$ NMR solvent), 6.97 (td, $^{3}J_{HH}$ = 8.0, $^{4}J_{HH}$ = 0.9, 1H, H^7), 6.67 (ddd, $^{3}J_{PtH}$ = 52.4,$^{3}J_{HH}$ = 7.4, $^{4}J_{HH}$ = 0.8,

View Article Online
DOI: 10.1039/C6RA21756G

$^4J_{PH}$ = 3.9, 1H, H^9), 6.52 (td, $^3J_{HH}$ = 8.0, $^4J_{HH}$ = 1.4, 1H, H^8). ^{31}P {^1H} NMR (162 MHz, $CDCl_3$, 20 °C, δ): 22.7 (s, $^1J_{PtP}$ = 4328, 1P).

Method B: To a yellow suspension of complex **1a** (100 mg, 0.14 mmol) in acetone (15 mL) was added a solution of Br_2 (36 µlit, 0.70 mmol, 5 equiv.) in acetone (5 mL) at room temperature. A fast color change to red was observed. The resulting solution was stirred for 2 h. Then, the solvent was reduced under vacuum to a small volume (1 mL) and *n*-hexane (5 mL) was added to precipitate complex **2b** as a green powder (61 mg, 64%).

Method C: To a green suspension of complex **A** (100 mg, 0.15 mmol) in acetone/CH_2Cl_2 (10:5 mL) was added an excess of KBr (53.6 g, 0.45 mmol, 3 equiv.) in acetone (2 mL) at room temperature. The resulting mixture was allowed to react while stirring for 30 h. Then, the solvent was removed under reduced pressure and the solid residue was extracted with CH_2Cl_2 (20 mL). The obtained green solution was filtered through Celite and the filtrate was concentrated to a small volume (1 mL). Finally, *n*-hexane (5 mL) was added to yield complex **2b** as a green solid (39 mg, 38%).

[Pt(ppy)(PPhMe$_2$)I], 2c.

To an orange solution of complex **1c** (100 mg, 0.17 mmol) in acetone (15 mL) was added an excess of MeI (208.3 μL, 3.4 mmol, 20 equiv.) at room temperature. The solution color turned red instantly and the mixture was stirred for 1 h. Then, the solvent was removed under reduced pressure and the resulting residue was triturated with *n*-hexane (3 × 2 mL). Finally, the resulting green solid was dried under vacuum. Yield: 64 mg, 62%. Elem. Anal. Calcd for $C_{19}H_{19}INPPt$ (614.32): C, 37.15; H, 3.12; N, 2.28; Found: C, 37.31; H, 3.24; N, 2.21. ^1H NMR (400 MHz, acetone-d_6, 20 °C, δ): 10.41 (m, $^3J_{PtH}$ = 32.3, 1H, H^2), 8.10-8.05 (m, 4H, H^4, H^5 and H^o of $PPhMe_2$), 7.70 (dd, $^3J_{HH}$ = 7.7, $^4J_{HH}$ = 1.4, 1H, H^6), 7.51-7.43 (m, 4H, H^3, H^p and H^m of $PPhMe_2$), 7.05 (td, $^3J_{HH}$ = 7.7, $^4J_{HH}$ = 1.1, 1H, H^7), 6.84 (ddd, $^3J_{PtH}$ = 55.3,$^3J_{HH}$ = 7.6, $^4J_{HH}$ = 1.0, $^4J_{PH}$ = 3.8, 1H, H^9), 6.77 (td, $^3J_{HH}$ = 7.7, $^4J_{HH}$ = 1.3, 1H, H^8), 2.21 (d, $^2J_{PH}$ = 10.8, $^3J_{PtH}$ = 39.9 Hz, 6H, Me group of $PPhMe_2$). ^{31}P {^1H} NMR (162 MHz, acetone-d_6, 20 °C, δ): -9.0 (s, $^1J_{PtP}$ = 4108, 1P).

View Article Online
DOI: 10.1039/C6RA21756G

[{Pt(ppy)(PPh$_3$)}$_2$(μ$_2$-Spy)]PF$_6$, 3-PF$_6$.

To a solution of complex **A** (100 mg, 0.15 mmol) in CH_2Cl_2 (15 mL) was added $AgPF_6$ (51 mg, 0.20 mmol). The reaction mixture was stirred for 5 h in dark at room temperature, and then filtered through Celite to remove AgCl. The green filtrate was treated with complex **1a** (108.3 mg, 0.15 mmol) in CH_2Cl_2 (5 mL). The resulting orange solution was stirred for 2 h and then the solvent was removed under reduced pressure and concentrated to a small volume (~ 1 mL) and *n*-hexane (3 mL) was added to obtain complex **3-PF$_6$**. Yield: 157 mg, 71%; m.p. 217 ˚C. MS ESI(+): *m/z* 1332.27 $[M\text{-}PF_6]^+$. Elem. Anal. Calcd for $C_{63}H_{50}F_6N_3P_3Pt_2S$ (1477.22): C, 51.18; H, 3.41; N, 2.84; Found: C, 51.47; H, 3.52; N, 2.91. ^{1}H NMR (400 MHz, $CDCl_3$, 20 °C, δ): 8.97 (m, $^3J_{PtH}$ = 32.7, 2H, H^2), 7.98-6.31 (overlapping multiplets, 48 H). ^{31}P {^{1}H} NMR (162 MHz, CD_2Cl_2, 20 °C, δ): 21.5 (s, $^1J_{PtP}$ = 4407, 1P, P^a *cis* with nitrogen atom of Spy ligand), 21.0 (s, $^1J_{PtP}$ = 4245, 1P, P^b *cis* with sulfur atom of Spy ligand), -144.4 (septet, $^1J_{PF}$ = 712, 1P, P of PF_6). ^{195}Pt {^{1}H} NMR (85.7 MHz, CD_2Cl_2, 20 °C, δ): -4081 (d, $^1J_{PtP}$ = 4413, 1Pt, Pt^a bound to the nitrogen atom of Spy ligand), -4296 (d, $^1J_{PtP}$ = 4256, 1Pt, Pt^b bound to the sulfur atom of Spy ligand).

Monitoring the Reaction of complexes 1a-c with electrophilic reagents (MeI, CD$_3$I, Br$_2$ and I$_2$) by ^{1}H and ^{31}P {^{1}H} NMR Spectroscopy.

To a solution of complexes **1a-c** (0.014 mmol) in CD_2Cl_2 (0.75 mL) in an NMR tube was added the appropriate electrophilic reagent at 298 K (0.020 mmol) or at 223 K (0.42 mmol). The tube was then placed in the probe of the NMR spectrometer, and NMR spectra were obtained at appropriate time intervals.

Crystal Structure Determination and Refinement. The X-ray diffraction measurements were carried out on STOE IPDS-2/2T diffractometer with graphite-monochromated Mo Kα radiation. All single crystals were mounted on a glass fiber and used for data collection. Cell constants and an orientation matrix for data collection were obtained by least-square refinement of the diffraction data from 4977, 4763, 4350 and 10828 for **A**, **2a**, **2b** and **3-PF$_6$**, respectively. Diffraction data were collected in a series of ω scans in 1˚ oscillations and integrated using the Stoe X-AREA[73] software package. A numerical absorption correction was applied using X-

View Article Online
DOI: 10.1039/C6RA21756G

RED[74] and X-SHAAPE[75] software. The data were corrected for Lorentz and polarizing effects. The structures were solved by direct methods[76] and subsequent difference Fourier maps and then refined on F^2 by a full-matrix least-squares procedure using anisotropic displacement parameters.[77] Atomic factors are from the International Tables for X-ray Crystallography.[78] All non-hydrogen atoms were refined with anisotropic displacement parameters. Hydrogen atoms were placed in ideal positions and refined as riding atoms with relative isotropic displacement parameters. A view of the structure is depicted in Figure 3 (top) and Figure S6. All refinements were performed using the X-STEP32, SHELXL-2014 and WinGX-2013.3 programs.[79-86] Also, the suitable crystals were obtained from $CHCl_3$/*n*-hexane solution (complexes **A**, **2a** and **2b**) or CH_2Cl_2/*n*-hexane solution (complex **3-PF$_6$**) at room temperature.

Theoretical Methods. Gaussian 09 was used[87] to fully optimize all the structures at the DFT/B3LYP level of density functional theory. The solvation energies were calculated by CPCM model in acetone. The effective core potential of Hay and Wadt with a double-x valence basis set (LANL2DZ) was chosen to describe Pt and I.[88] The 6-31G(d) basis set was used for other atoms.

Electronic supplementary information (ESI) available: NMR spectra, crystallographic and computational details (PDF). Crystallographic data (CIF).

Acknowledgments

This work was supported by the Institute for Advanced Studies in Basic Sciences (IASBS) Research Council. Technical support of the Chemistry Computational Center at Shahid Beheshti University is gratefully acknowledged. Thanks are also due to Dr. F. Niroomand Hosseini, Islamic Azad University (Shiraz Branch), for helpful assistance and discussions on DFT calculations, Dr. A. Neshat, IASBS, for valuable suggestions, Mr. A. Biglari, the operator of Bruker NMR instrument at IASBS, for recording the NMR spectra and Prof. Elena Lalinde, Universidad de La Rioja, for ESI-MS measurements.

References

View Article Online
DOI: 10.1039/C6RA21756G

1. M. Golbon Haghighi, S. M. Nabavizadeh, M. Rashidi and M. Kubicki, *Dalton Trans.*, 2013, **42**, 13369-13380.
2. D. M. Crumpton-Bregel and K. I. Goldberg, *J. Am. Chem. Soc.*, 2003, **125**, 9442-9456.
3. H. R. Shahsavari, M. Rashidi, S. M. Nabavizadeh, S. Habibzadeh and F. W. Heinemann, *Eur. J. Inorg. Chem.*, 2009, 3814-3820.
4. Á. Molnár, *Chem. Rev.*, 2011, **111**, 2251-2320.
5. Á. Molnár, in *Palladium-Catalyzed Coupling Reactions: Practical Aspects and Future Developments*, Wiley-VCH Verlag GmbH & Co. KGaA, 2013.
6. J. M. Brown and N. A. Cooley, *Chem. Rev.*, 1988, **88**, 1031-1046.
7. P. G. Gildner and T. J. Colacot, *Organometallics*, 2015, **34**, 5497-5508.
8. J. F. Hartwig, *Inorg. Chem.*, 2007, **46**, 1936-1947.
9. J. F. Hartwig, *Nature*, 2008, **455**, 314-322.
10. J. Racowski and M. Sanford, in *Higher Oxidation State Organopalladium and Platinum Chemistry*, ed. A. J. Canty, Springer Berlin Heidelberg, 2011, vol. 35, pp. 61-84.
11. K. A. Grice, M. L. Scheuermann and K. I. Goldberg, in *Higher Oxidation State Organopalladium and Platinum Chemistry*, ed. A. J. Canty, Springer, 2011, vol. 35, pp. 1-38.
12. A. V. Pawlikowski, A. D. Getty and K. I. Goldberg, *J. Am. Chem. Soc.*, 2007, **129**, 10382-10393.
13. A. R. Dick, J. W. Kampf and M. S. Sanford, *J. Am. Chem. Soc.*, 2005, **127**, 12790-12791.
14. T. Kondo and T.-a. Mitsudo, *Chem. Rev.*, 2000, **100**, 3205-3220.
15. C. Shen, P. Zhang, Q. Sun, S. Bai, T. S. A. Hor and X. Liu, *Chem. Soc. Rev.*, 2015, **44**, 291-314.
16. I. P. Beletskaya and V. P. Ananikov, *Chem. Rev.*, 2011, **111**, 1596-1636.
17. S. V. Ley and A. W. Thomas, *Angew. Chem. Int. Ed.*, 2003, **42**, 5400-5449.
18. J. Zhang, C. M. Medley, J. A. Krause and H. Guan, *Organometallics*, 2010, **29**, 6393-6401.
19. E. Traversa, J. L. Templeton, H. Y. Cheng, M. Mohadjer Beromi, P. S. White and N. M. West, *Organometallics*, 2013, **32**, 1938-1950.
20. M. Mellah, A. Voituriez and E. Schulz, *Chem. Rev.*, 2007, **107**, 5133-5209.
21. A. R. Murphy and J. M. J. Fréchet, *Chem. Rev.*, 2007, **107**, 1066-1096.
22. G. Liu, J. R. Huth, E. T. Olejniczak, R. Mendoza, P. DeVries, S. Leitza, E. B. Reilly, G. F. Okasinski, S. W. Fesik and T. W. von Geldern, *J. Med. Chem.*, 2001, **44**, 1202-1210.
23. M. Niazi, H. R. Shahsavari, M. Golbon Haghighi, M. R. Halvagar, S. Hatami and B. Notash, *RSC Adv.*, 2016, **6**, 76463-76472.
24. H. Samouei, M. Rashidi and F. W. Heinemann, *J. Iran. Chem. Soc.*, 2014, **11**, 1207-1216.
25. N. Furukawa, F. Takahashi, T. Kawai, K. Kishimoto, S. Ogawa and S. Oae, *Phosphorus, Sulfur, Silicon Relat. Elem.*, 1983, **16**, 167-180.
26. S. Fuertes, A. J. Chueca and V. Sicilia, *Inorg. Chem.*, 2015, **54**, 9885-9895.
27. L. Rigamonti, C. Manassero, M. Rusconi, M. Manassero and A. Pasini, *Dalton Trans.*, 2009, 1206-1213.
28. J. C. Schug, J. W. Viers and J. I. Seeman, *J. Org. Chem.*, 1983, **48**, 4892-4899.
29. P. Beak and J. T. Lee, *J. Org. Chem.*, 1969, **34**, 2125-2128.

View Article Online
DOI: 10.1039/C6RA21756G

30. M. Dadkhah Aseman, S. M. Nabavizadeh, H. R. Shahsavari and M. Rashidi, *RSC Adv.*, 2015, **5**, 22692-22702.
31. M. S. McCready and R. J. Puddephatt, *Organometallics*, 2015, **34**, 2261-2270.
32. T. Schaefer and J. D. Baleja, *J. Magn. Reson.*, 1984, **60**, 131-135.
33. R. Babadi Aghakhanpour, S. M. Nabavizadeh, L. Mohammadi, S. Amini Jahromi and M. Rashidi, *J. Organomet. Chem.*, 2015, **781**, 47-52.
34. L. Maidich, A. Zucca, G. J. Clarkson and J. P. Rourke, *Organometallics*, 2013, **32**, 3371-3375.
35. A. Zucca, L. Maidich, L. Canu, G. L. Petretto, S. Stoccoro, M. A. Cinellu, G. J. Clarkson and J. P. Rourke, *Chem. Eur. J.*, 2014, **20**, 5501-5510.
36. L. F. Lindoy, S. E. Livingstone and T. N. Lockyer, *Inorg. Chem.*, 1967, **6**, 652-656.
37. L. F. Lindoy and S. E. Livingstone, *Inorg. Chem.*, 1968, **7**, 1149-1154.
38. J. J. Stace, P. J. Ball, V. Shingade, S. Chatterjee, A. Shiveley, W. L. Fleeman, A. J. Staniszewski, J. A. Krause and W. B. Connick, *Inorg. Chim. Acta*, 2016, **447**, 98-104.
39. A. K. Fazlur-Rahman and J. G. Verkade, *Inorg. Chem.*, 1992, **31**, 5331-5335.
40. D. G. VanDerveer and R. Eisenberg, *J. Am. Chem. Soc.*, 1974, **96**, 4994-4996.
41. A. Vlčk Jr, *Inorg. Chim. Acta*, 1980, **43**, 35-42.
42. W. B. Connick and H. B. Gray, *J. Am. Chem. Soc.*, 1997, **119**, 11620-11627.
43. R. Zanella, R. Ros and M. Grazian, *Inorg. Chem.*, 1973, **12**, 2736-2738.
44. M. S. Chernov'yants, I. V. Burykin, Z. A. Starikova and N. E. Erofeev, *J. Mol. Struc.*, 2011, **1006**, 379-382.
45. C.-H. Cheng, B. D. Spivack and R. Eisenberg, *J. Am. Chem. Soc.*, 1977, **99**, 3003-3011.
46. C.-H. Cheng and R. Eisenberg, *Inorg. Chem.*, 1979, **18**, 2438-2445.
47. J. K. Jawad, F. N. K. Al-Obaidy, J. A. Hammud and F. Al-Azab, *J. Organomet. Chem.*, 2000, **599**, 166-169.
48. V. Sicilia, M. Baya, P. Borja and A. Martín, *Inorg. Chem.*, 2015, **54**, 7316-7324.
49. S. M. Nabavizadeh, H. Amini, F. Jame, S. Khosraviolya, H. R. Shahsavari, F. Niroomand Hosseini and M. Rashidi, *J. Organomet. Chem.*, 2012, **698**, 53-61.
50. P. Hamidizadeh, M. Rashidi, S. M. Nabavizadeh, M. Samaniyan, M. Dadkhah Aseman, A. M. Owczarzak and M. Kubicki, *J. Organomet. Chem.*, 2015, **791**, 258-265.
51. J. R. Berenguer, E. Lalinde, A. Martín, M. T. Moreno, S. Ruiz, S. Sánchez and H. R. Shahsavari, *Inorg. Chem.*, 2014, **53**, 8770-8785.
52. Á. Díez, E. Lalinde and M. T. Moreno, *Coord. Chem. Rev.*, 2011, **255**, 2426-2447.
53. A. Esmaeilbeig, H. Samouei, S. Abedanzadeh and Z. Amirghofran, *J. Organomet. Chem.*, 2011, **696**, 3135-3142.
54. A. Díez, J. Forniés, A. García, E. Lalinde and M. T. Moreno, *Inorg. Chem.*, 2005, **44**, 2443-2453.
55. A. Zucca, G. L. Petretto, S. Stoccoro, M. A. Cinellu, M. Manassero, C. Manassero and G. Minghetti, *Organometallics*, 2009, **28**, 2150-2159.
56. P. K. Byers and A. J. Canty, *Organometallics*, 1990, **9**, 210-220.
57. M. Gholinejad and H. R. Shahsavari, *Inorg. Chim. Acta*, 2014, **421**, 433-438.
58. D. Black, G. Deacon and G. Edwards, *Aust. J. Chem.*, 1994, **47**, 217-227.
59. E. S. Tabei, H. Samouei and M. Rashidi, *Dalton Trans.*, 2011, **40**, 11385-11388.
60. C. Janiak, *J. Chem. Soc., Dalton Trans.*, 2000, 3885-3896.

View Article Online
DOI: 10.1039/C6RA21756G

61. M. Ferrer, D. Gómez-Bautista, A. Gutiérrez, G. Orduña-Marco, L. A. Oro, J. J. Pérez-Torrente, O. Rossell and E. Ruiz, *Organometallics*, 2016, **35**, 336-345.
62. R. Babadi Aghakhanpour, M. Rashidi, F. Niroomand Hosseini, F. Raoof and S. M. Nabavizadeh, *RSC Adv.*, 2015, **5**, 66534-66542.
63. F. Raoof, M. Boostanizadeh, A. R. Esmaeilbeig, S. M. Nabavizadeh, R. Babadi Aghakhanpour, K. B. Ghiassi, M. M. Olmstead and A. L. Balch, *RSC Adv.*, 2015, **5**, 85111-85121.
64. S. M. Nabavizadeh, F. Niroomand Hosseini, N. Nejabat and Z. Parsa, *Inorg. Chem.*, 2013, **52**, 13480-13489.
65. K. I. Goldberg, J. Yan and E. M. Breitung, *J. Am. Chem. Soc.*, 1995, **117**, 6889-6896.
66. R. H. Crabtree, in *The Organometallic Chemistry of the Transition Metals*, John Wiley & Sons, Inc., 6th edn., 2014.
67. U. Fekl and K. I. Goldberg, *Adv. Inorg. Chem.*, 2003, **54**, 259.
68. K. I. Goldberg, J. Y. Yan and E. L. Winter, *J. Am. Chem. Soc.*, 1994, **116**, 1573-1574.
69. B. S. Williams, A. W. Holland and K. I. Goldberg, *J. Am. Chem. Soc.*, 1999, **121**, 252-253.
70. B. S. Williams and K. I. Goldberg, *J. Am. Chem. Soc.*, 2001, **123**, 2576-2587.
71. J. Procelewska, A. Zahl, G. Liehr, R. van Eldik, N. A. Smythe, B. S. Williams and K. I. Goldberg, *Inorg. Chem.*, 2005, **44**, 7732-7742.
72. B. S. Furniss, A. J. Hannaford, P. W. G. Smith and A. R. Tatchell, *Vogel's Textbook of Practical Organic Chemistry*, 5th edn., Longman Scientific & Technical, 1989.
73. Stoe & Cie, X–AREA: Program for the Acquisition and Analysis of Data, Version 1.30; Stoe & Cie GmbH: Darmatadt, Germany, 2005.
74. Stoe & Cie, X–RED: Program for Data Reduction and Absorption Correction, Version 1.28b; Stoe & Cie GmbH: Darmatadt, Germany, 2005.
75. Stoe & Cie, X–SHAPE: Program for Crystal Optimization for Numerical Absorption Correction, Version 2.05; Stoe & Cie GmbH: Darmatadt, Germany, 2004.
76. Sheldrick, G. M. SHELX97. Program for Crystal Structure Solution. University of Göttingen, Germany, 1997.
77. Sheldrick, G. M. SHELX97. Program for Crystal Structure Refinement. University of Göttingen, Germany, 1997.
78. E. Prince, International Tables for X-ray Crystallography, Vol C, Kluwer Academic Publisher, Doordrecht, The Netherlands, 1995.
79. F. H. Allen, O. Johnson, G. P. Shields, B. R. Smith and M. Towler, *J. Appl. Cryst.*, 2004, **37**, 335-338.
80. L. J. Farrugia, *J. Appl. Cryst.*, 1999, **32**, 837-838.
81. C. F. Macrae, P. R. Edgington, P. McCabe, E. Pidcock, G. P. Shields, R. Taylor, M. Towler and J. van der Streek, *J. Appl. Cryst.*, 2006, **39**, 453-457.
82. Burnett, M. N.; Johnson, C. K. ORTEP-III Report ORNL-6895. Oak Ridge National Laboratory, Tennessee, USA 1996.
83. A. L. Spek, *J. Appl. Cryst.*, 2003, **36**, 7-13.
84. G. M. Sheldrick, *Acta Crystallogr., Sect. A*, 2008, **64**, 112-122.
85. P. Coppens, L. Leiserowitz and D. Rabinovich, *Acta Crystallogr.*, 1965, **18**, 1035-1038.

View Article Online
DOI: 10.1039/C6RA21756G

86. , Stoe & Cie, X-STEP32: Crystallographic Package, Version 1.07b; Stoe & Cie GmbH: Darmstadt, Germany, 2000.
87. M. J. Frisch, G. W. Trucks, H. B. Schlegel, G. E. Scuseria, M. A. Robb, J. R. Cheeseman, G. Scalmani, V. Barone, B. Mennucci, G. A. Petersson, H. Nakatsuji, M. Caricato, X. Li, H. P. Hratchian, A. F. Izmaylov, J. Bloino, G. Zheng, J. L. Sonnenberg, M. Hada, M. Ehara, K. Toyota, R. Fukuda, J. Hasegawa, M. Ishida, T. Nakajima, Y. Honda, O. Kitao, H. Nakai, T. Vreven, J. J. A. Montgomery, J. E. Peralta, F. Ogliaro, M. Bearpark, J. J. Heyd, E. Brothers, K. N. Kudin, V. N. Staroverov, T. Keith, R. Kobayashi, J. Normand, K. Raghavachari, A. Rendell, J. C. Burant, S. S. Iyengar, J. Tomasi, M. Cossi, N. Rega, J. M. Millam, M. Klene, J. E. Knox, J. B. Cross, V. Bakken, C. Adamo, J. Jaramillo, R. Gomperts, R. E. Stratmann, O. Yazyev, A. J. Austin, R. Cammi, C. Pomelli, J. W. Ochterski, R. L. Martin, K. Morokuma, V. G. Zakrzewski, G. A. Voth, P. Salvador, J. J. Dannenberg, S. Dapprich, A. D. Daniels, O. Farkas, J. B. Foresman, J. V. Ortiz, J. Cioslowski and D. J. Fox, *Gaussian 09, Revision B.01*, 2010.
88. P. J. Hay and W. R. Wadt, *J. Chem. Phys.*, 1985, **82**, 270-283.

View Article Online
DOI: 10.1039/C6RA21756G

Table of Contents Entry

Carbon–Sulfur Bond Reductive Coupling from a Platinum(II) Thiolate Complex

Complex [Pt(ppy)(η^1-S-Spy)(PPh_3)], **1**, was reacted with different electrophilic alkyl halide reagents at room temperature. This reaction proceeded *via* formation of binuclear intermediate complex [{Pt(ppy)(PPh_3)}$_2$(μ_2-Spy)]$^+$, **3**, and through C–S bond reductive coupling to produce alkyl sulfides and corresponding halide complexes [Pt(ppy)(PPh_3)X], **2**, X = I, Br.